Road Centerline Extraction via Semi-supervised Segmentation and Multidirection Non-maximum Suppression

Guangliang Cheng, Feiyun Zhu, Shiming Xiang and Chunhong Pan

***Abstract*—Accurate road centerline extraction from remotely sensed images plays a significant role in road map generation and updating. In the road extraction problem, acquisition of labeled data is time-consuming and costly, thus there are only a small amount of labeled samples in reality. In the existing centerline extraction algorithms, the thinning based algorithms always produce small spurs that reduce the smoothness and accuracy of the road centerline; the regression based algorithms can extract smooth road network, while they are time-consuming. To solve the above problems, we propose a novel road centerline extraction method, which is constructed based on semi-supervised segmentation and multiscale filtering (MF) & multidirection non-maximum suppression (M-NMS). Specifically, a semi-supervised method, which explores the intrinsic structures between the labeled samples and the unlabeled ones, is introduced to obtain the segmentation result. Then, a novel MF&M-NMS based algorithm is proposed to gain smooth and complete road centerline network. Experimental results on a public dataset demonstrate that the proposed method achieves comparable or better performances by comparing with state-of-the-art methods. In addition, our method is nearly 10 times faster than state-of-the-art methods.**

***Index Terms*—road centerline extraction, semi-supervised segmentation, multiscale filtering (MF), multidirection non-maximum suppression (M-NMS).**

I. Introduction

ROAD centerline extraction from remotely sensed imagery has been an active research due to its vital applications in urban planning, vehicle navigation and intelligent transportation system, etc. Although various approaches [1], [2], [3] have been proposed to address this task, it is still challenging to obtain both smooth and complete road network.

For most existing road centerline extraction methods [4], [5], [6], two steps are included to obtain the final road network. First, different kinds of algorithms are employed to obtain the homogenous road area result. Then a centerline extraction algorithm is used to get the final road centerline network.

In the road area extraction problem, supervised classification algorithms [4], [7], [8] were widely used. A support vector machine (SVM) based road network extraction method was proposed by Shi et al. [4], in which spectral-spatial classification and shape features were employed. Cheng et al. [7] presented a graph cuts based road extraction approach, in which SVM based probability propagation and spatial information were integrated. Mnih et al. [8] proposed a deep neural network based method to extract urban road network from high-resolution images. Although these supervised classification based methods have achieved great results, a large amount of labeled samples are needed to train these classifiers. However, manually labeled samples are expensive and difficult to acquire. Actually, in most cases, we only have a small set of labeled samples and a large collection of unlabeled ones.

For the road centerline extraction problem, morphological thinning algorithm [5], [6] was widely used because it is fast and easy to implement. However, the thinning based algorithm always produces short spurs and brings in many false positives, which reduce the smoothness and accuracy of the road network. To alleviate these problems, some regression based centerline extraction algorithms [4], [9] have been introduced. Although these algorithms can extract smooth and accurate road centerlines, they also have two shortcomings: 1) they are ineffective to extract the centerlines around the road intersections; 2) they are time-consuming.

To solve the problem of limited labeled samples, inspired by Nie et al. [10], we propose a semi-supervised road area extraction algorithm, which incorporates the information of both labeled and unlabeled samples. Then, to overcome the above shortcomings of centerline extraction algorithms, a multiscale filtering & multidirection non-maximum suppression (MF&M-NMS) algorithm is proposed. The main contributions of our approach are highlighted as follows:

1. A new semi-supervised road area extraction algorithm is proposed. By exploring the intrinsic structures between the labeled samples and unlabeled ones, it greatly improves the road extraction performance with limited labeled samples.

2. A novel MF&M-NMS based road centerline extraction algorithm is proposed. On the one hand, this algorithm can extract smooth road network with little processing time. On the other hand, it can overcome the shortcoming of existing regression based algorithms in the road intersections, thus it can obtain complete road network.

The remainder of this letter is arranged as follows. Section II presents the proposed methodology. Experimental evaluations and detailed comparisons are reported in Section III. Conclusions are drawn in Section IV.

Manuscript received September 10, 2015; revised December 13, 2015 and January 26, 2016; accepted January 27, 2016. Date of publication XXXXX; date of current version XXXXXX. This work was supported by the Natural Science Foundation of China under Grants 91338202, 91438105, 61305049 and 61370039.

The authors are with the National Laboratory of Pattern Recognition, Institute of Automation, Chinese Academy of Sciences, Beijing 100190, China (e-mail: {guangliang.cheng, fyzhu, smxiang and chpan}@nlpr.ia.ac.cn).

Color versions of one or more of the figures in this paper are available online at http://ieeexplore.ieee.org.

II. The Proposed Methodology

The proposed road extraction approach consists of three steps: object-based feature extraction, semi-supervised segmentation and MF&M-NMS based road centerline extraction.

A. Object-based Feature Extraction

In this letter, to reduce the side influence of occlusions and to extract the geometric characteristics of road regions, the object-oriented algorithm is employed to extract the contextual features of road regions. Though other choices are also feasible, here we use the Mean Shift [11] algorithm to generate superpixels, which are treated as objects. Mean shift runs fast and can preserve the road boundaries well.

In this letter, inspired by Cheng et al. [12], we utilize three types of features: spectral features, geometric & texture features, and contextual features. They are defined as follows.

Spectral features: As the pixels within one superpixel tend to have similar spectral characteristics, thus we define the spectral attribute of a superpixel as the average spectral value within this superpixel.

Geometric & texture features: The extended multi-attribute profile (EMAP) [13] was widely used to capture the geometric and texture features in hyperspectral image analysis. EMAP captures the spatial information via morphological attribute filters, such as area, diagonal of the bounding box of the region, etc. Here we extract the EMAP features for all the pixels in the image, then we calculate the EMAP feature of a superpixel as the mean value of the EMAP features in this superpixel.

It should be noted that we normalize the above two features, respectively. Then we concatenate them as the feature of the superpixel. To enhance the discriminative power of each superpixel, the spatially adjacent superpixels should be considered, which is defined as contextual information as follows.

Contextual features: Intuitively, road regions are connected together. In most cases, for a road superpixel, there are at least two road superpixels in its spatially neighboring superpixels. Among all the spatially neighboring superpixels of the center superpixel, we find out the two superpixels, which are the first two closest superpixels to the center superpixel in concatenated feature space. Then we concatenate them as the contextual feature for the center superpixel.

B. Semi-supervised Segmentation

Suppose we have obtained N superpixels after oversegmentation. For clarity, we denote the i-th superpixel by $\mathbf{x}_i \in \mathbb{R}^m$ $(i = 1, 2, ...N)$, where m is the dimension of the features. In semi-supervised learning, only limited labeled samples are available. Without loss of generality, suppose the first l samples $\mathbf{x}_1, \mathbf{x}_2, ...\mathbf{x}_l$ are labeled and the others are unlabeled. Denote $\mathbf{X} = [\mathbf{x}_1, \mathbf{x}_2, ...\mathbf{x}_N] \in \mathbb{R}^{m\times N}$ as the feature matrix for all the samples. For the two-class classification problem, we denote the label of the positive samples (road class) as 1 and -1 for the negative samples (non-road class). Let $\mathbf{f}_{(l)} = [y_1, y_2, ...y_l]^T$ denote the label vector of the labeled samples. For those unlabeled samples, we denote its initial label as 0. Let $\mathbf{f}_{(u)}$ denote the predicted label vector for those unlabeled samples. Denote the predicted label vector by $\mathbf{f} = \begin{bmatrix} \mathbf{f}_{(l)} \\ \mathbf{f}_{(u)} \end{bmatrix} \in \mathbb{R}^N$.

Problem formalization: In our method, the road segmentation problem is studied in a semi-supervised framework via regression based algorithm. The model can be described as follows:

$$\arg\min_{\mathbf{w},\mathbf{f},b} \sum_{i=1}^{l} ||\mathbf{w}^T\mathbf{x}_i + b - y_i||_2^2 + \lambda \sum_{i=l+1}^{N} ||\mathbf{w}^T\mathbf{x}_i + b - y_i||_2^2 + \alpha(\mathbf{f}^T\mathbf{L}\mathbf{f}) + \beta||\mathbf{w}||_2^2, \tag{1}$$

where $\mathbf{w} \in \mathbb{R}^m$ and b are projection vector and bias scatter, respectively; λ, α and β are hyperparameters, where λ controls the relative significance of the labeled samples and the unlabeled samples. $\mathbf{L} \in \mathbb{R}^{N\times N}$ is a Laplacian matrix on the graph, which is calculated by $\mathbf{L} = \mathbf{D} - \mathbf{S}$. $\mathbf{S}$ is a similarity matrix, which is calculated to encode the similarity between sample pairs via *k-nearest neighbor* (*k*-NN) and heat kernel function [14]. $\mathbf{D}$ is a diagonal matrix, whose i-th diagonal element is calculated by $d_{ii} = \sum_j s_{ij}$. The first term and the second term in Eq. 1 are regression errors for the labeled samples and unlabeled ones, respectively. The third term is a graph based manifold regularization, which is to enhance the label smoothness between the samples. The regularization term $||\mathbf{w}||_2^2$ is used to avoid overfitting.

In Eq. 1, the first two terms can be combined, thus a concise formulation can be defined as

$$\mathcal{L} = (\mathbf{X}_a^T\mathbf{w}_a - \mathbf{f})^T\mathbf{\Lambda}(\mathbf{X}_a^T\mathbf{w}_a - \mathbf{f}) + \alpha(\mathbf{f}^T\mathbf{L}\mathbf{f}) + \beta\mathbf{w}_a^T\mathbf{w}_a, \tag{2}$$

where $\mathbf{X}_a = [\mathbf{X}; \mathbf{1}^T] \in \mathbb{R}^{(m+1)\times N}$ is an augmented matrix, in which $\mathbf{1}$ is a vector with all the elements as one; Accordingly, $\mathbf{w}_a = [\mathbf{w}; b] \in \mathbb{R}^{m+1}$ is an augmented vector; $\mathbf{\Lambda} = \text{diag}\{1, 1, ...\lambda, \lambda\} \in \mathbb{R}^{N\times N}$ is a diagonal weight matrix for all the samples.

The objective function in Eq. 2 is convex and differentiable with respect to $\mathbf{f}$ and $\mathbf{w}_a$. Thus, the optimum is expected to be achieved. In this letter, an iterative update algorithm is employed to find the optimal solution.

Optimization: Fixing $\mathbf{f}$, taking the derivative of $\mathcal{L}$ with respect to $\mathbf{w}_a$, we obtain

$$\frac{\partial\mathcal{L}}{\partial\mathbf{w}_a} = 2\mathbf{X}_a\mathbf{\Lambda}\mathbf{X}_a^T\mathbf{w}_a - 2\mathbf{X}_a\mathbf{\Lambda}\mathbf{f} + 2\beta\mathbf{w}_a. \tag{3}$$

Let $\partial\mathcal{L}/\partial\mathbf{w}_a = 0$, we get

$$\mathbf{w}_a = \left(\mathbf{X}_a\mathbf{\Lambda}\mathbf{X}_a^T + \beta\mathbf{I}_{(m+1)}\right)^{-1}\mathbf{X}_a\mathbf{\Lambda}\mathbf{f} \tag{4}$$

where $\mathbf{I}_{(m+1)}$ is a $(m+1)\times(m+1)$ identity matrix.

Fixing $\mathbf{w}_a$, taking the derivative of $\mathcal{L}$ with respect to $\mathbf{f}$, we obtain

$$\frac{\partial\mathcal{L}}{\partial\mathbf{f}} = -2\mathbf{\Lambda}\mathbf{X}_a^T\mathbf{w}_a + 2\mathbf{\Lambda}\mathbf{f} + 2\alpha\mathbf{L}\mathbf{f}. \tag{5}$$

Let $\partial\mathcal{L}/\partial\mathbf{f} = 0$, we obtain

$$\mathbf{f} = \left(\mathbf{\Lambda} + \alpha\mathbf{L}\right)^{-1}\mathbf{\Lambda}\mathbf{X}_a^T\mathbf{w}_a. \tag{6}$$

Algorithm 1 : Semi-supervised road segmentation.

Input:

The object-based feature matrix of the image $\mathbf{X}_a$;
The label vector for the labeled instances $\mathbf{f}_{(l)}$;
Parameter λ, α and β.

Output:

Pixel-based road segmentation result.

Initialize $\mathbf{f}$ and $\mathbf{w}_a$.
Calculate the graph based Laplacian matrix $\mathbf{L}$.
repeat
  Update $\mathbf{w}_a$ by the updating rule (4).
  Update $\mathbf{f}$ by the updating rule (6).
until Convergence
Obtain the object-based label via Eq. (7).
Obtain the pixel-based label according to the rule (II-B).
return Pixel-based road segmentation result.

By iteratively updating $\mathbf{w}_a$ and $\mathbf{f}$, when the changes of the two values lie within a very small scope, the optimization process converges.

After the iterative update, we get the predicted label matrix. Then we classify an unlabeled sample $\mathbf{x}_i$ $(l+1 < i < N)$ with a threshold τ (usually we set $\tau = 0$) according to the following rule:

$$l(\mathbf{x}_i) = \begin{cases} 1 & \text{if } f(\mathbf{x}_i) \geq \tau \\ -1 & \text{else} \end{cases}. \tag{7}$$

After obtaining the final labels for all the superpixels, all the pixel labels are obtained according to the rule II-B: All the pixels in the same superpixel are given the same label value as the superpixel. The semi-supervised road segmentation algorithm is summarized in Algorithm 1.

After the segmentation, many road-like segments (i.e. roofs and parking lots, etc) are also included in the final segmentation result. To distinguish between potential road segments and road-like segments, the elimination algorithm with road-geometrical prior [7] is employed. After this process, only the road segments are remained.

C. Road Centerline Extraction via Multiscale Filtering & Multidirection Non-maximal Suppression

In the road centerline extraction problem, traditional morphological thinning algorithm was widely used, because it is fast and easy to implement. However, it always produces short spurs and brings in many false positives. To overcome this shortcoming, regression based algorithms [4], [9] were performed to obtain smooth road centerlines, while they are time-consuming. To solve above problems, an MF&M-NMS based road centerline extraction algorithm is proposed. It has two strengths: a) It does not produce spurs. b) It is fast and easy to be realized.

Multiscale filtering: For the segmentation result, we continuously filter the image with different kernel size. Specifically, at the first, we filter the image with larger filter size, then we use the filters in the declining size. This is behind the motivation that after above continuous filtering, the real road centerline positions tend to have local maximum values. Thus the multiscale filtering can be defined as

$$\mathbf{I}^{(s+1)} = \mathbf{I}^{(s)} * \mathbf{F}^{(s+1)}, \tag{8}$$

where s denotes the s-th filtering, $\mathbf{I}^{(0)}$ denotes the segmentation result without any filtering; $*$ denotes the convolution operation; $\mathbf{F}$ denotes the convolution kernel, here we use the gaussian kernel. Intuitively, the maximal kernel size should be larger than the road width, and then we decrease the kernel size to 3 at the step of 2. After that, local maximum values accumulate to road centerline positions. As Fig. 1(b) shows, the centerline positions are lighter than the surrounding areas. Thus, it demonstrates that the multiscale filtering algorithm is effective to accumulate the maximum values to road centerline positions.

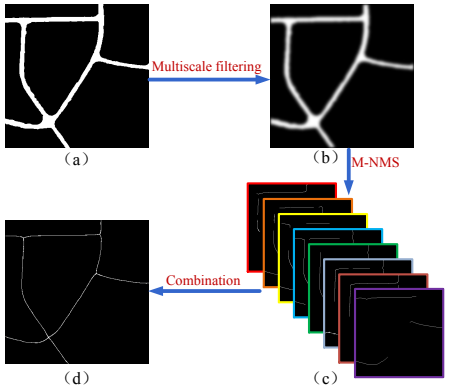

Fig. 1. The flowchart of the proposed road centerline extraction method. (a) Road segmentation result. (b) Result after multiscale filtering. (c) Result after multidirection non-maximum suppression. (d) Final centerline result.

Multidirection non-maximum suppression: To get the complete and smooth road centerline network, non-maximum suppression (NMS) algorithm is applied. The NMS only remains those locations, which are the local maximum along a line perpendicular to the local orientation within a neighborhood of width. We found that the road network is incomplete when only using one certain orientation. Thus, in our experiments, we use the NMS in 8 different orientations $(0, 45°, 90°, 135°, 180°, 225°, 270°, 315°)$. As Fig. 1(c) shows, we obtain road centerline results from 8 different NMS orientations. As we can see, though some centerline parts are detected more than once, these 8 centerline extraction results complement with each other.

Combination: After we have obtained 8 road centerline extraction results, a combination rule should be proposed to integrate these results. Here we combine the results according to the following rules:

1) We eliminate the centerlines with less than T pixels. Because roads are continuous and connected with each other, thus short centerlines tend to be non-road part.
2) Only those locations, which are detected more than twice, are remained on the final road centerline network.

After the above process, we get the final road centerline network. As Fig. 1(d) shows, the centerline network is smooth and complete by employing the MF&M-NMS algorithm.

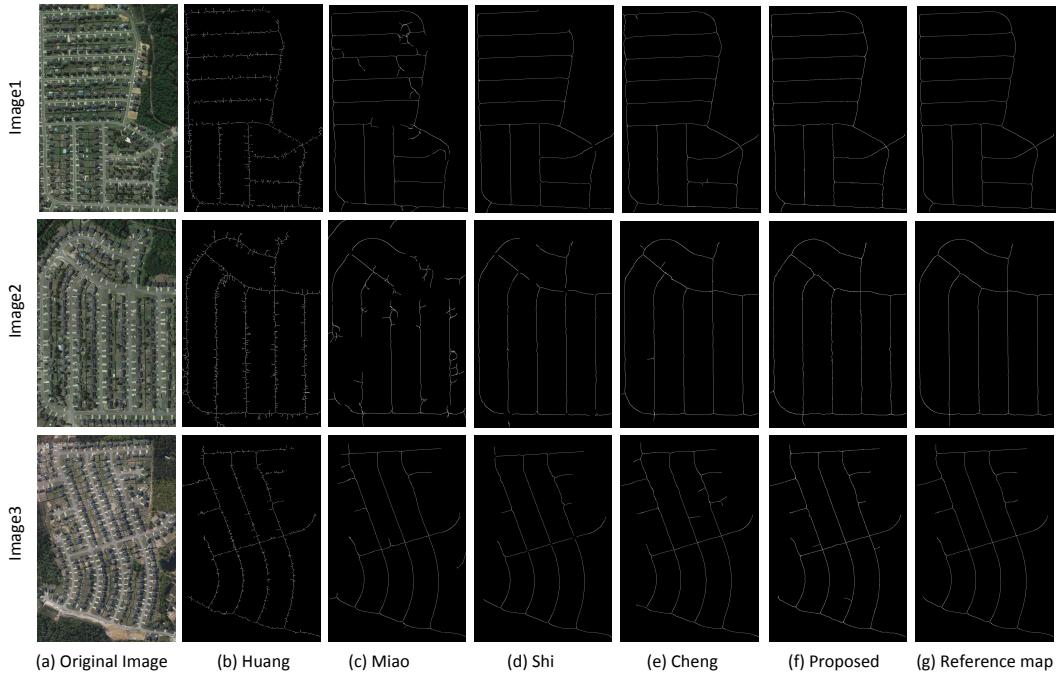

Fig. 2. Visual comparisons of road centerline extraction results. From left to right: (a) original image, (b) result of Huang [5], (c) result of Miao [9], (d) result of Shi [4], (e) result of Cheng [12], (f) result of Proposed, (g) the reference map. (Due to the space limit, we only display three images)

III. Experimental Results

To verify the effectiveness of our method, visual and quantitative performances are compared with other state-of-the-art methods. Due to the space limit, we only display three images.

A. Datasets

We use the road centerline extraction dataset provided by Cheng et al. [12] to test the proposed method. In this dataset, there are 30 images with the spatial resolution of $1.2m$ per pixel. Most of the images are under complex backgrounds and occlusions of cars and trees.

B. Compared Methods

To test the performances of the proposed method, we compared our approach with state-of-the-art road centerline extraction methods. They are Huang's method (Huang) [5], Miao's method (Miao) [9], Shi's method (Shi) [4] and Cheng's method (Cheng) [12].

C. Quality Evaluation

To evaluate the performance of road centerline extraction methods, *completeness* (com), *correctness* (cor) and *quality* (q) [15] are used in this letter. Due to the deviation between the manually labeled centerline and the real centerline, "buffer width" [16] is introduced to calculate these metrics. In the experiments, we set the buffer width as 2 pixels.

D. Parameter Setting

For mean shift, we set $(h_s, h_r, M) = (7, 5, 100)$, where h_s and h_r are bandwidth parameters in the spatial and range domains, and M is the minimum size of each superpixel. In our experiments, we set $\beta = 1$. Intuitively, the relative importance of the unlabeled samples should be smaller than the labeled samples, thus we set $\lambda = 0.6$. We tune the parameter α via cross validations. In the MF step, we employ the filtering window size from 19 to 3 at the interval of 2 pixels. In the M-NMS step, we set the window size of NMS as 20 and $T = 10$ for all the experiments.

TABLE I
Quantitative comparisons among different methods, where the values in bold text are the best and the values in bold italic text are the second best. It should be noted that the last column is the average performance of all images in dataset.

		Huang	Miao	Shi	Cheng	Proposed
Image1	com	*0.9763*	0.9064	0.9204	0.9651	**0.9885**
	cor	0.6362	0.7801	**0.9791**	*0.9370*	0.9212
	q	0.6265	0.7219	0.9027	*0.9063*	**0.9114**
Image2	com	0.9732	0.7532	0.8250	*0.9891*	**0.9967**
	cor	0.5714	0.6014	**0.9762**	*0.9442*	0.9236
	q	0.5625	0.5024	0.8087	**0.9345**	*0.9208*
Image3	com	*0.9911*	0.9701	0.9250	0.9592	**0.9935**
	cor	0.7421	0.9151	**0.9534**	*0.9382*	0.9184
	q	0.7372	0.8900	0.8850	*0.9022*	**0.9129**
Avg(dataset)	com	*0.9353*	0.8578	0.8973	0.9228	**0.9427**
	cor	0.6827	0.8176	**0.9109**	*0.9078*	0.8946
	q	0.6505	0.7200	0.8249	*0.8437*	**0.8485**

E. Performance Evaluation

Visual comparisons: Fig. 2 shows the comparing results of different methods in visual performance. Cheng's method and the proposed method gain better performance than other three methods. Huang's method produces more small spurs than other methods. Miao's method produces some false

TABLE II
TIME COMPARISONS OF DIFFERENT METHODS, HERE THE TIME IS MEASURED IN SECONDS. **Ct** REFERS TO THE AVERAGE **C**LASSIFICATION **t**IME, AND **Et** REFERS TO THE AVERAGE CENTERLINE **E**XTRACTION **t**IME.

	Image1		Image2		Image3	
size	1316*738		999*692		1232*735	
	Ct(s)	**Et**(s)	**Ct**(s)	**Et**(s)	**Ct**(s)	**Et**(s)
Huang	251.76	0.08	115.18	0.06	253.51	0.07
Miao	22.72	298.54	14.58	240.32	19.56	246.87
Shi	80.72	305.42	60.27	245.37	68.35	253.61
Cheng	249.70	247.51	197.35	190.35	235.73	195.73
Proposed	45.89	22.73	35.53	19.35	42.95	29.10

positives, because it is hard for this method to distinguish the homogenous areas from real road areas. In addition, Miao's method and Shi's method are not effective to extract the centerlines in the road intersections.

Quantitative comparisons: Table I shows the quantitative performance of the sample images and average performance of all the 30 images in the dataset. As we can see, the proposed method is comparable to or better than Cheng's method, which gains best performance among the comparing methods. Huang's method and Miao's method obtain relatively poor results because there are a lot of false positives.

In the experiments, the number of labeled samples used in Huang's method and Cheng's method are 200 and 100, respectively. While the proposed method only need 60 labeled samples. Shi's method utilizes 5% of the number of all the pixels. It demonstrates that our semi-supervised based method can achieve better performance with less labeled samples.

F. Time Comparison

The average running time among different methods in the classification stage and the centerline extraction stage are illustrated in Table II. All the experiments are conducted on a computer with Intel Core i5-3470 3.20GHz CPU and 8GB RAM using Matlab 2013. The result does not include the cross validation time. As can be seen from the table, Miao's method and the proposed method take less time than other three methods in the classification stage. Huang's method and Cheng's method take more time in this stage, this is because they are multiscale based methods. In the road centerline extraction stage, Huang's method takes the least time. While it produces short spurs around the centerline, thus reducing the smoothness and accuracy of the centerline. Miao's method, Shi's method and Cheng's method cost more than 10 times running time of the proposed method. Thus, it demonstrates that the proposed method acieves relatively better performance with less running time than other state-of-the-art methods.

IV. CONCLUSIONS

In this letter, a fast and easily implemented method has been proposed to extract road centerlines from remotely sensed imagery. In terms of both visual and quantitative performances, the proposed method achieves better results than all the other comparing methods. Moreover, the proposed road centerline extraction algorithm was 10 times faster than those regression based algorithms.

Actually, the proposed method can be also applied to other images, such as multispectral or hyperspectral images. However, there are some limits to the proposed method. First, the proposed method has good performance on rural roads and suburban roads, while as with other methods, the performance may decrease on the urban road images. Second, although the proposed method can connect the short discontinuity, it can not effectively infer or connect the long discontinuity, which is an open question in the centerline extraction task.

REFERENCES

[1] M.-F. Auclair Fortier, D. Ziou, C. Armenakis, and S. Wang, "Survey of work on road extraction in aerial and satellite images," *Technical Report*, vol. 24, no. 16, pp. 3037–3058, May 2003.

[2] J. B. Mena, "State of the art on automatic road extraction for GIS update: a novel classification," *Pattern Recognit. Lett.*, vol. 24, no. 16, pp. 3037–3058, Apr. 2003.

[3] A. Kaur and E. Ram Singh, "Various methods of road extraction from satellite images: A review," *Int. J. of Research*, vol. 02, no. 02, pp. 1025–1032, Nov. 2014.

[4] W. Shi, Z. Miao, and J. Debayle, "An integrated method for urban main-road centerline extraction from optical remotely sensed imagery," *IEEE Trans. Geosci. Remote Sens.*, vol. 52, no. 6, pp. 3359–3372, Jun. 2014.

[5] X. Huang and L. Zhang, "Road centreline extraction from high resolution imagery based on multiscale structural features and support vector machines," *Int. J. of Remote Sens.*, vol. 30, no. 8, pp. 1977–1987, Apr. 2009.

[6] W. Shi, Z. Miao, Q. Wang, and H. Zhang, "Spectral-spatial classification and shape features for urban road centerline extraction," *IEEE Geosci. Remote Sens. Lett.*, vol. 11, no. 4, pp. 788–792, Apr. 2014.

[7] G. Cheng, Y. Wang, Y. Gong, F. Zhu, and C. Pan, "Urban road extraction via graph cuts based probability propagation," in *IEEE Int. C. Image Processing*, Oct. 2014, pp. 5072–5076.

[8] V. Mnih and G. E. Hinton, "Learning to detect roads in high-resolution aerial images," in *European Conference on Computer Vision*, Sep. 2010, pp. 210–223.

[9] Z. Miao, W. Shi, H. Zhang, and X. Wang, "Road centerline extraction from high-resolution imagery based on shape features and multivariate adaptive regression splines," *IEEE Geosci. Remote Sens. Lett.*, vol. 10, no. 3, pp. 583–587, May 2013.

[10] F. Nie, H. Wang, H. Huang, and C. H. Q. Ding, "Adaptive loss minimization for semi-supervised elastic embedding," in *IJCAI*, Aug. 2013.

[11] D. Comaniciu and P. Meer, "Mean shift: A robust approach toward feature space analysis," *IEEE Trans. Pattern Anal. Mach. Intell.*, vol. 24, no. 5, pp. 603–619, May 2002.

[12] G. Cheng, F. Zhu, S. Xiang, and C. Pan, "Accurate urban road centerline extraction from vhr imagery via multiscale segmentation and tensor voting." [Online]. Available: http://arxiv.org/pdf/1508.06163.pdf

[13] D. Mura, Mauro, J. Benediktsson, B. Waske, and L. Bruzzone, "Extended profiles with morphological attribute filters for the analysis of hyperspectral data," *Int. J. of Remote Sens.*, vol. 31, no. 22, pp. 5975–5991, Dec. 2010.

[14] W. Dong, M. Charikar, and K. Li, "Efficient k-nearest neighbor graph construction for generic similarity measures," in *WWW*, Apr. 2011, pp. 577–586.

[15] C. Heipke, H. Mayer, C. Wiedemann, and O. Jamet, "Evaluation of automatic road extraction," in *International Archives of Photogrammetry and Remote Sensing*, Feb. 1997, pp. 47–56.

[16] B. Wessel and C. Wiedemann, "Analysis of automatic road extraction results from airborne sar imagery," in *ISPRS Archives*, Sep. 2003, pp. 105–110.